



## Conversion of elemental mercury with a novel membrane catalytic system at low temperature

Yongfu Guo<sup>a,b</sup>, Naiqiang Yan<sup>a,\*</sup>, Shijian Yang<sup>a</sup>, Ping Liu<sup>a</sup>, Juan Wang<sup>a</sup>, Zan Qu<sup>a</sup>, Jinping Jia<sup>a</sup>

<sup>a</sup> School of Environmental Science and Engineering, Shanghai Jiao Tong University, Shanghai, 200240, PR China

<sup>b</sup> Department of Municipal Engineering, Suzhou University of Science and Technology, Suzhou, 215011, PR China

### ARTICLE INFO

#### Article history:

Received 26 October 2011

Received in revised form 15 January 2012

Accepted 16 January 2012

Available online 23 January 2012

#### Keywords:

Flue gas

Elemental mercury

Catalytic oxidation

MnO<sub>x</sub>

Catalyst

### ABSTRACT

A unique assembly, which integrated membrane delivery for oxidants with catalytic oxidation (MDCOs), was employed to convert elemental mercury (Hg<sup>0</sup>) to its oxidized form at low temperature (around 150 °C). MnO<sub>x</sub> was used as the main catalytic component in MDCOs with Mo and/or Ru to improve the catalytic activity. The MDCOs was proved to be very effective for the conversion of Hg<sup>0</sup> compared with the traditional catalytic oxidation mode (TCO). The analysis of speciation for Hg after catalytic oxidation showed that there was mainly mercury (II) chloride. The addition of transition metals of Mo and Ru obviously improved the conversion of Hg<sup>0</sup> to Hg<sup>2+</sup> and enhanced the activity of the MDCOs at low temperature, and the conversion efficiency of Hg<sup>0</sup> reached 95% with Mo-Ru-Mn catalyst and 8 ppmv HCl. The inhibition of SO<sub>2</sub> to Hg<sup>0</sup> conversion in the MDCOs was insignificant. The Hg<sup>0</sup> removal exceeded 80% even if the concentration of SO<sub>2</sub> reached 1000 ppmv. The results also indicated that the Deacon reaction with the yield of Cl<sub>2</sub> were significantly improved after modified, and MDCOs with Mo-Ru-Mn catalyst can work efficiently at low temperature.

© 2012 Elsevier B.V. All rights reserved.

## 1. Introduction

Mercury (Hg) is one of the most concerned heavy metal contaminants, and coal combustion is an important emission source for atmospheric mercury [1,2]. Hg emission from coal-fired flue gas often presents in three main forms: elemental (Hg<sup>0</sup>), gaseous divalent (Hg<sup>2+</sup>) and particulate-associated (Hg(p)) [3], in which Hg<sup>0</sup> is the most difficult to be captured with the existing air pollution control devices [4].

Hg<sup>0</sup> in flue gases can be oxidized by HCl in the presence of certain catalysts. However, most of the investigated catalysts for this purpose can only work efficiently at higher temperature, such as above 523 K [5,6]. Thus these catalysts have to work upstream of air-preheater and particulate collection devices to meet such temperature window, where the deterioration of the catalyst by the high content of flyash in flue gas was often encountered [7]. In addition, the traditional catalytic oxidation mode (TCO) exists some shortcomings for Hg<sup>0</sup> oxidation [8,9]. First of all, Hg<sup>0</sup> in flue gas is just at the trace level (1–5 μg m<sup>-3</sup>) [10], but the large amount of oxidants are needed to obtain high removal efficiency. Therefore, the efficiency of oxidants is rather low now for the most tested TCO

modes. Moreover, introducing too much of oxidants into flue gas may bring the risk of secondary effect.

In order to overcome the shortcomings of TCO mentioned above, we have put forward a unique technology that integrated the membrane delivery and catalytic oxidation (MDCOs) for Hg<sup>0</sup> conversion at low temperature. The MDCOs used porous ceramic membrane doped with transition metals as catalyst. Based on the series of our previous experiments [11], it is found that the MDCOs system with MnO<sub>x</sub> as the main catalytic component was very effective for Hg<sup>0</sup> conversion and displayed excellent sulfur-tolerant at the temperature of 573 K [11]. And the employed efficiency of oxidants is higher in the MDCOs. However, the performance of the MDCOs at low temperature is still unclear.

Furthermore, although some transition metal oxides (e.g., MnO<sub>x</sub>) showed excellent performance for Hg<sup>0</sup> conversion at high temperature [11–15], most were less active at low temperature and SO<sub>2</sub> had significantly negative effect on Hg<sup>0</sup> conversion. Based on our preliminary tests [13], the activity of transition metal catalysts could be significantly enhanced by doping some metal oxides, such as molybdenum (Mo) or ruthenium (Ru).

Therefore, in order to well understand the performance of the MDCOs at low temperature, the conversion efficiency of Hg<sup>0</sup>, efficiency of oxidants, the influence of catalyst composition and the different components of flue gas were mainly investigated. Meanwhile, the catalysts of MnO<sub>x</sub> and MnO<sub>x</sub> modified with Mo and/or

\* Corresponding author. Tel.: +86 21 54745591; fax: +86 21 54745591.  
E-mail address: [nqyan@sjtu.edu.cn](mailto:nqyan@sjtu.edu.cn) (N. Yan).

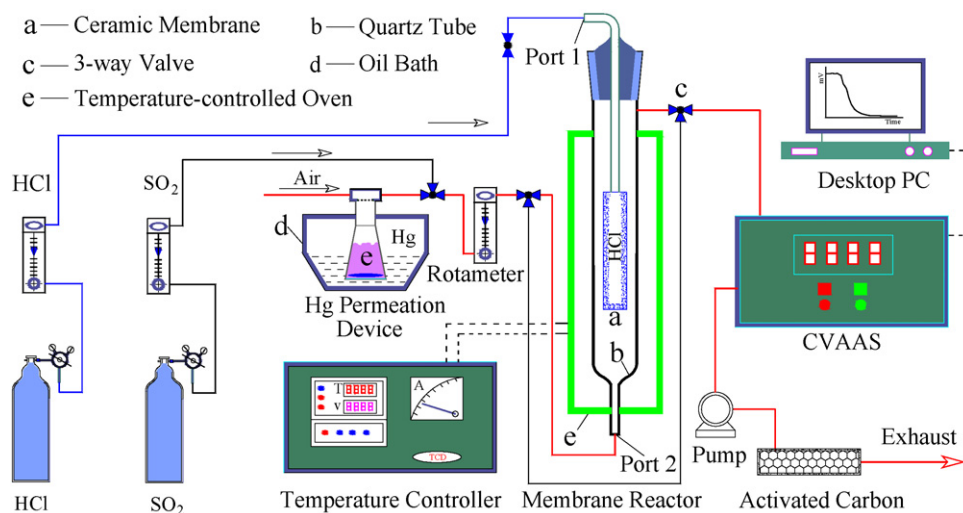


Fig. 1. Experimental scheme of the MDCOs system.

Ru were prepared and characterized together with their catalytic properties.

## 2. Experimental

### 2.1. Experimental assembly

The experimental assembly is shown in Fig. 1, which was used to evaluate the performance of  $\text{Hg}^0$  conversion in the MDCOs system. The MDCOs reactor consisted of a quartz tube (360 mm in length with an inner diameter of 16 mm) and a tubular ceramic membrane mounted coaxially. The CVAAS (SG-921, Jiangfen Ltd.) was used to continuously monitor and acquire the inlet ( $C_0$ ) or outlet ( $C$ )  $\text{Hg}^0$  concentration of the reactor. The measurement for HCl,  $\text{Cl}_2$  and  $\text{SO}_2$  was carried out with the recommended method of gas detector tubes (Gastec, Japan).

As shown in Fig. 1, the injection of HCl from port 1 was considered as the MDCOs process. In addition, the process can be regarded as the TCO mode if HCl was injected from port 2, where HCl would be premixed with the simulated flue gas before contacting with catalysts.

### 2.2. Catalyst preparation

The MDCOs system employed a porous tubular membrane that was made of alumina ( $\text{Al}_2\text{O}_3$ , Hefei Great Wall Co. Ltd.), with pore diameter of  $4.7 \mu\text{m}$ , inner diameter of 8 mm, outer diameter of 12 mm, Brunauer–Emmett–Teller (BET) surface of  $4.1 \text{ m}^2 \text{ g}^{-1}$  and length of 50 mm. The catalysts were prepared by wet impregnation method and expressed as M or M–Mn, in which M represented the doped metals, i.e., Mn, Mo, Ru, Mo–Mn, Ru–Mn or Mo–Ru–Mn. The loading value of manganese to  $\text{Al}_2\text{O}_3$  was set at  $8 (\pm 0.2) \text{ wt.}\%$  as default value in later experiments. The loading values of Mo and Ru to Mn were set at 1 mol% and 0.5 mol%, respectively. All chemicals, including the precursors of  $\text{Mn}(\text{NO}_3)_2$ ,  $(\text{NH}_4)_6\text{Mo}_7\text{O}_{24} \cdot 4\text{H}_2\text{O}$  and  $\text{RuCl}_3 \cdot 3\text{H}_2\text{O}$ , used for catalyst preparation were of analytical grade, and purchased from Sino-pharm Chemical Reagent Co.

### 2.3. Test conditions

The experiments were performed in the MDCOs at the temperature of 423 K with the simulated flue gas of  $\text{SO}_2$  and/or HCl. Air was mixed as the source of  $\text{O}_2$ . All the gases were monitored with rotameters, and the total flow rate was set at  $25.0 \text{ L h}^{-1}$ . The flow

rates of  $\text{SO}_2$  and HCl were set at 2.0 and  $1.0 \text{ L h}^{-1}$ , respectively. The continuous operation time before acquire the data was set at 4 h at all tests if it was not clearly stated.

### 2.4. Analysis of sample characterization

The X-ray diffractometer (XRD, D/max-2200/PC, Rigaku Co., Japan) was used to determine the crystal structures of catalysts at 40 kV and 20 mA using  $\text{Cu K}\alpha$  radiation in the range of  $20\text{--}80^\circ$  ( $2\theta$ ) with a step size of  $0.02^\circ$ . The analysis of oxide specimens was performed with an X-ray photoelectron spectroscopy (XPS, PHI-5000C ESCA). The morphology of catalysts was scanned by a field emission scanning electron microscope (FE-SEM, SIRION 200, USA). An energy dispersive X-ray spectrometer (EDX, INCA OXFORD) was used to examine the distribution of doped element in catalysts.

## 3. Results

### 3.1. Removal of $\text{Hg}^0$ in MDCOs and TCO mode with Mn catalyst

Fig. 2 illustrates the removal of  $\text{Hg}^0$  in the MDCOs and TCO mode with Mn catalyst under various conditions. The results showed that the removal efficiencies of  $\text{Hg}^0$  in the TCO mode were far less than that in the MDCOs mode both at 423 K and 573 K. The removal efficiency of  $\text{Hg}^0$  in the TCO mode hardly reached 60% even if 20 ppmv HCl was used at 573 K (Fig. 2(b)). In Fig. 2(a), it also shows that the removal efficiency of  $\text{Hg}^0$  can reach 80% or higher in the MDCOs mode with the presence of 12 ppmv HCl. Compared with the removal of  $\text{Hg}^0$  in the two modes, it was obvious that the MDCOs mode had obvious superiority at the removal of  $\text{Hg}^0$  over the TCO mode at low temperature. However,  $\text{Hg}^0$  conversion efficiency in MDCOs just with Mn as the catalyst was not high enough at low temperature even increasing the concentration of HCl to 20 ppmv. Therefore, it was necessary to further enhance the catalyst activity in MDCOs at low temperature.

### 3.2. Performance of catalytic oxidation with modified Mn catalysts

The elemental mercury conversion efficiencies with various transition metals are shown in Fig. 3. It can be seen that the activity of Mn catalyst was greatly improved after modification with Mo or Ru, and Mo–Ru–Mn catalyst had an optimal improvement on the removal of  $\text{Hg}^0$  with efficiency of 95%. The analysis of Hg speciation

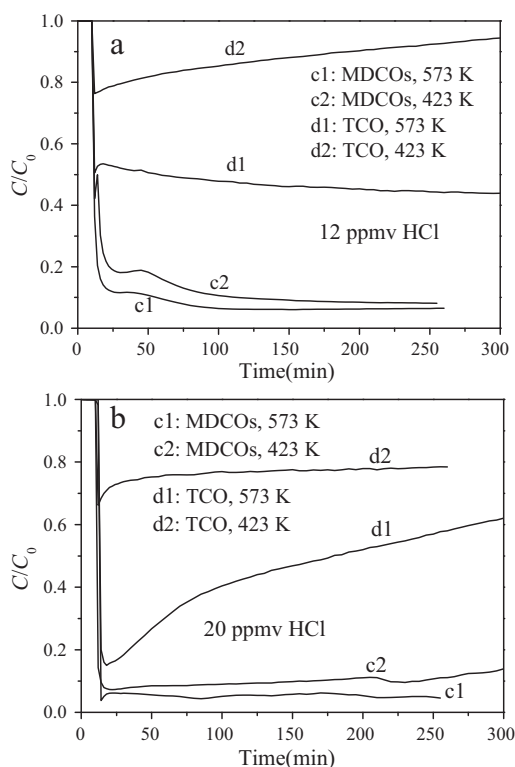


**Fig. 2.** Removal efficiencies of  $\text{Hg}^0$  with Mn catalyst in the MDCOs and TCO mode at different conditions. Reaction conditions:  $[\text{SO}_2] = 0$ ,  $C_0$  was about 24.2 ppbv, and air was used as carrier gas.

showed that the proportion of mercury (II) chloride on the catalysts of Mn, Mo-Mn, Ru-Mn and Mo-Ru-Mn accounted for 63%, 71%, 91% and 93%, respectively. The results showed that the addition of transition metals of Mo and Ru can obviously increase the conversion of  $\text{Hg}^0$  to  $\text{Hg}^{2+}$  in the MDCOs. Compared with Mn catalyst, the conversion of  $\text{Hg}^0$  with Mo-Ru-Mn catalyst increased by 30%. As shown in Figs. 2 and 3, the removal of  $\text{Hg}^0$  in MDCOs with Mo-Ru-Mn cannot only improve the conversion of  $\text{Hg}^0$  but also save the amount of oxidants at low temperature of 423 K. It was also found that  $\text{O}_2$  played an important role on the  $\text{Hg}^0$  removal. When high purity  $\text{N}_2$  was used as the carrier gas without oxygen, weak Hg removal was detected with efficiency of about 8% with Mn catalyst being present.

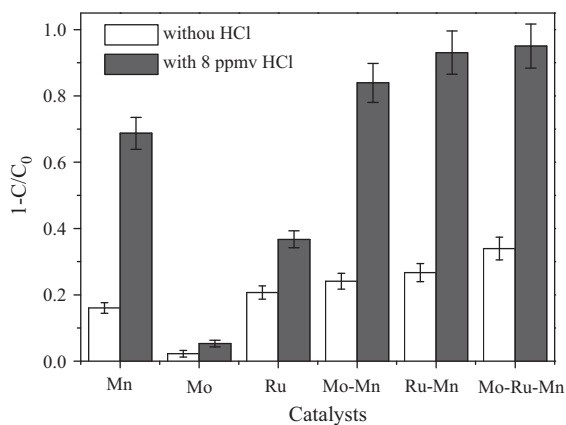


**Fig. 3.** Removal efficiencies of  $\text{Hg}^0$  with the catalysts doped with various transition metals in the MDCOs mode. Reaction conditions:  $[\text{HCl}] = 8$  ppmv,  $[\text{SO}_2] = 0$ ,  $T = 423$  K,  $C_0$  was about 23.5 ppbv, and air was used as carrier gas.

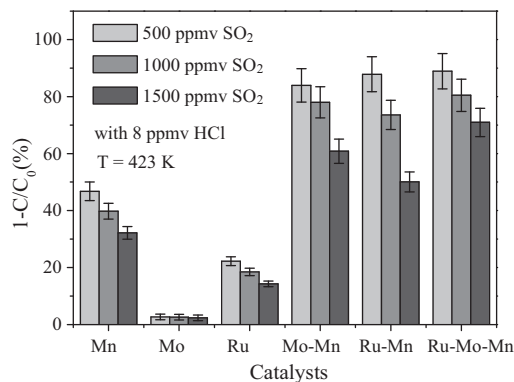


**Fig. 4.** Influence of  $\text{SO}_2$  on the removal of  $\text{Hg}^0$  with the catalysts doped with various transition metals at 423 K. Reaction conditions:  $[\text{HCl}] = 8$  ppmv,  $C_0$  was about 23 ppbv, and air was used as carrier gas.

### 3.3. Effect of $\text{SO}_2$ on $\text{Hg}^0$ removal

The results of gas-phase studies indicated that Mo and Ru had a promoting function for Mn catalyst on sulfur-tolerance to  $\text{SO}_2$  at the test conditions. Compared with Mn catalyst, the modified catalysts with Mo or Mo/Ru showed good sulfur-tolerance to  $\text{SO}_2$  (Fig. 4). The removal of  $\text{Hg}^0$  reached about 90% when 500 ppmv  $\text{SO}_2$  was introduced. The efficiency was far higher than that in the TCO mode shown in Fig. 2. Fig. 4 shows that the presence of  $\text{SO}_2$  suppressed the capacity of the MDCOs for  $\text{Hg}^0$  removal. However, the inhibition of  $\text{SO}_2$  was insignificant. The removal of  $\text{Hg}^0$  exceeded 80% even with 1000 ppmv of  $\text{SO}_2$ .

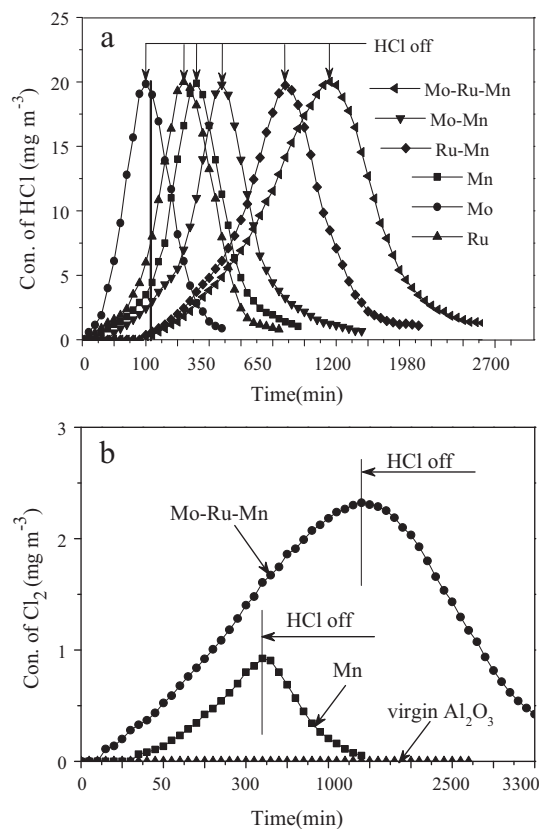


**Fig. 5.** Penetration curves of (a) HCl and (b)  $\text{Cl}_2$  produced in the MDCOs at 423 K without  $\text{Hg}^0$  in the gas. Reaction conditions: initial HCl concentration was about  $20 \text{ mg m}^{-3}$  with flow rate of  $2.0 \text{ L h}^{-1}$ .

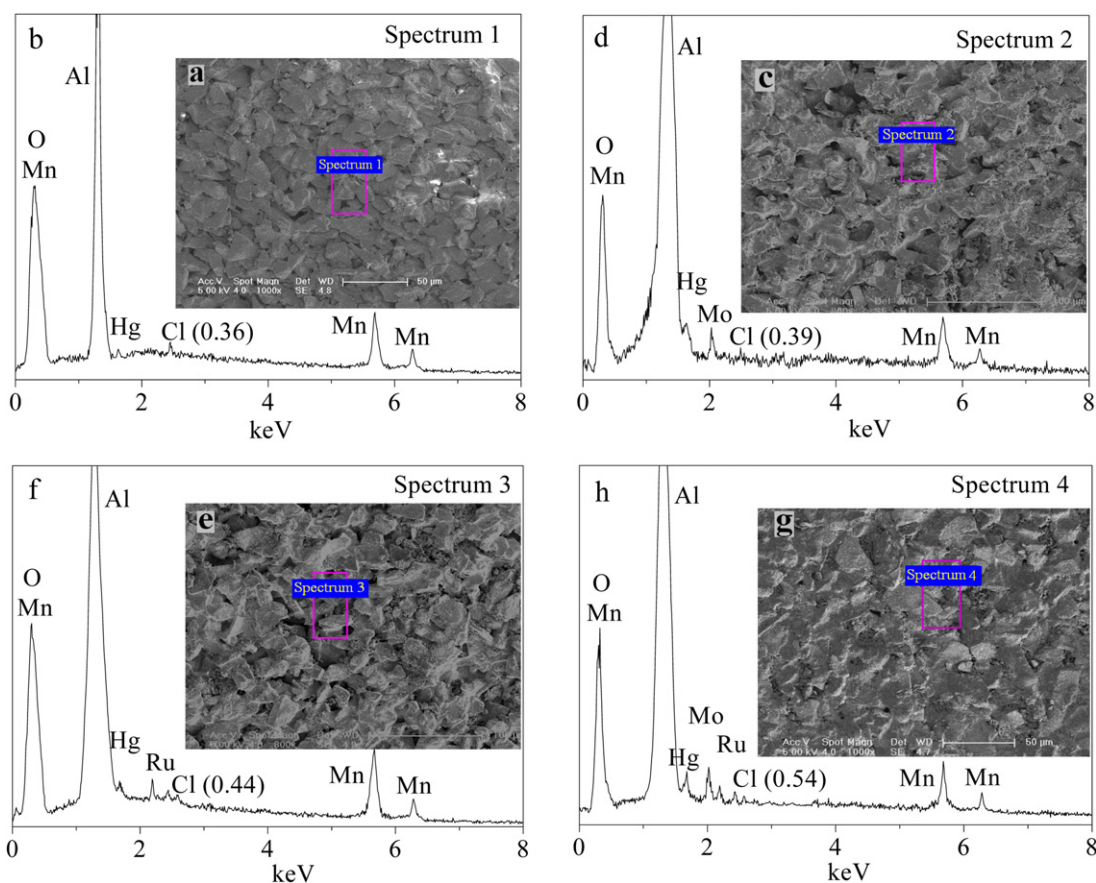


**Fig. 6.** FE-SEM and EDX spectra of the catalysts after HCl used. (a) and (b) Mn catalyst, (c) and (d) Mo-Mn catalyst, (e) and (f) Ru-Mn catalyst, and (g) and (h) Mo-Ru-Mn catalyst. The numbers in bracket are the contents of Cl (wt.%) on the surface of the catalysts. Reaction conditions: [HCl] = 8 ppmv, [SO<sub>2</sub>] = 0, C<sub>0</sub> was about 24 ppbv, and air was used as carrier gas.

According to the literature, the formation of HgSO<sub>4(ad)</sub> may be occur due to the chemical adsorption of SO<sub>2</sub> and further conversion [16]. To confirm the presence of HgSO<sub>4</sub>, the test analyzed the XPS spectrum of S 2p after SO<sub>2</sub> was used. On the basis of the result of S 2p XPS and combined with the spectra of Hg 4f and O 1s, it can be confirmed that Hg specie was assigned to HgSO<sub>4</sub> (BE 168.7 eV) by the XPS database of the National Institute of Standards and Technology (NIST) [17] and pervious literature [18].

### 3.4. Retainability and conversion of HCl

Previous studies have indicated that the Deacon process might be the predominant pathway for Hg<sup>0</sup> oxidation by HCl in the presence of catalysts [19,20], especially in the presence of Ru [21,22]. Moreover, chlorine (Cl<sub>2</sub>) and Cl atom (hydrogen abstracted from HCl) are active intermediates [5,23], and their yield can be used as an identifier to evaluate the efficiency of the Deacon process in the MDCOs. Even though Cl<sub>2</sub>/Cl concentration in coal-fired flue gas is very low, it is likely that Cl<sub>2</sub> is still in excess over Hg<sup>0</sup>.

In addition, the penetration curves of HCl in the MDCOs were investigated, and the results were shown in Fig. 5. As shown in Fig. 5(a), the ceramic membrane doped with unmodified MnO<sub>x</sub> displayed a significant retainability for HCl. The complete breakthrough time for Mn catalyst was about 6 h. And the retainability of ceramic membrane for HCl varied along with doped transition metals. Fig. 5(a) shows that Mo-Ru-Mn catalyst had the longest breakthrough time of 21 h, which might be favorable for the yield of Cl<sub>2</sub> and the conversion of Hg<sup>0</sup>. The adsorbed equilibrium amount of HCl on the surface of Mn and Mo-Ru-Mn catalysts were 28 and 98 μg-HCl/g-tube at 423 K, respectively.

On the basis of the tests in Fig. 5, the sorbed HCl in MDCOs with various catalysts can be evaluated. When Hg<sup>0</sup> removal reached stable (about 120 min, the vertical solid line in Fig. 5(a)), the amount of escaped HCl for Mn, Mo, Ru, Mo-Mn, Ru-Mn and Mo-Ru-Mn catalysts were 4.4, 19.0, 8.0, 3.0, 0.6 and 0.4 mg m<sup>-3</sup>, respectively. It can be seen that Mo-Ru-Mn catalyst had the lowest amount of escaped HCl (less than 2%).

The production of Cl<sub>2</sub>(g) in the MDCOs was also monitored along with HCl penetration across the membrane (Fig. 5(b)). It was

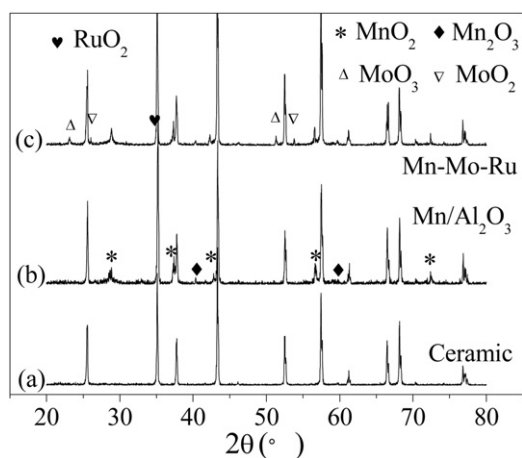


**Fig. 7.** X-ray diffraction patterns of (a) virgin ceramic tube, (b) Mn catalyst and (c) Mo-Ru-Mn catalyst.

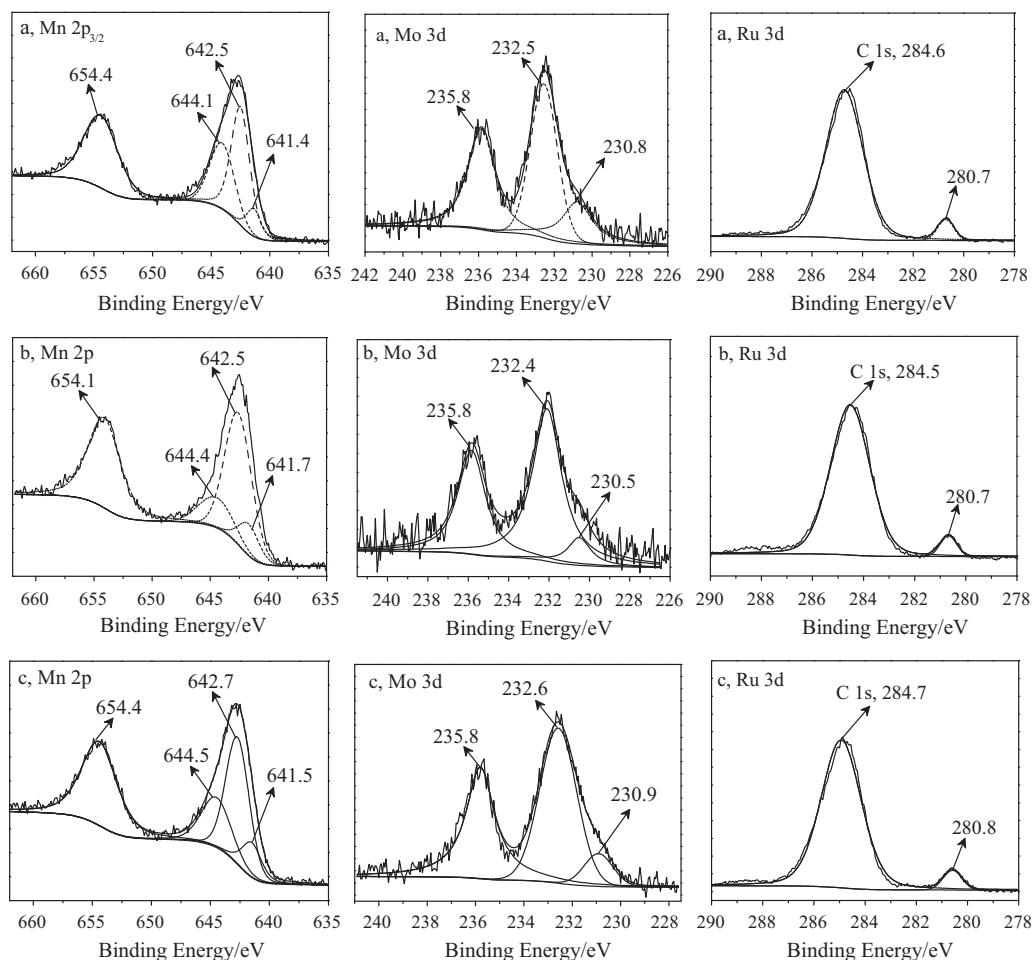


**Fig. 8.** XPS spectroscopies of Mn 2p, Mo 3d and Ru 3d (dash is fitted results). (a) Sample a, (b) sample b and (c) sample c. Mo-Ru-Mn catalyst was used. Air was used as carrier gas.

indicates that virgin ceramic membrane had no catalysis to the Deacon process. Though  $\text{Cl}_2$  can be hardly detected out in the TCO mode, a higher  $\text{Cl}_2$  yield was measured in the MDCOs and the maximum concentration of  $\text{Cl}_2$  was about  $2.3 \text{ mg m}^{-3}$  (curve of Mo-Ru-Mn in Fig. 5(b)). By Comparison with Mn and virgin  $\text{Al}_2\text{O}_3$  curves in Fig. 5(b), the  $\text{Cl}_2$  yield from Mn catalyst doubled after modified with Mo and Ru. The results show that the Deacon process was greatly accelerated after the MDCOs was modified with Mo and Ru, resulting in the increasing of  $\text{Cl}_2$  yield.

However, it is difficult to determine in situ the contents of atomic chlorine (reactive activated  $[\text{Cl}]^*$  produced from the Deacon process) or adsorbed  $\text{HgCl}_{(\text{ad})}$  at the tested conditions. The EDX spectra of the different catalysts after catalytic oxidation for  $\text{Hg}^0$  were used to analyze approximately the contents of atomic chlorine, and the results were shown in Fig. 6.

To eliminate the influence of chlorine derived from  $\text{RuCl}_3$ , the prepared catalysts were washed with 10 wt.%  $\text{NH}_4\text{OH}$  solution until both the XPS and EDX did not detected the existence of chlorine [24]. Fig. 6 shows that the amount (0.54 wt.%) of adsorbed Cl or  $\text{Cl}^-$  on Mo-Ru-Mn catalyst were more than that on Mn catalyst (0.26 wt.%), although we could not conclusively distinguish the speciation of Cl. It validates that the Deacon process was indeed accelerated after the MDCOs was modified with Mo or Ru.

### 3.5. Structural properties

The XRD patterns in Fig. 7(b) and (c) illustrate the primary diffraction peaks of manganese oxides, which are uniform with

those of  $\text{MnO}_2$  at  $2\theta = 28.68^\circ$ ,  $37.33^\circ$ ,  $42.83^\circ$ ,  $56.65^\circ$ , and  $72.26^\circ$  (JCPDS 24-0735), respectively [25]. It is obvious that  $\text{MnO}_x$  mainly presented in the form of  $\text{MnO}_2$  though the weak peak for  $\text{Mn}_2\text{O}_3$  could also be observed. The presence of  $\text{MoO}_3$  was confirmed by the diffraction peaks of the molybdenum (VI) at  $2\theta = 23.12^\circ$  and  $51.32^\circ$ , (JCPDS 47-1081). Simultaneously, the  $\text{MoO}_2$  was found at  $2\theta = 26.04^\circ$  and  $53.76^\circ$  (JCPDS 50-0739). Fig. 7(c) shows that the ruthenium speciation was attributed to  $\text{RuO}_2$ , based on the characteristic peaks of ruthenium at  $2\theta = 28.01^\circ$  (hardly shown) and  $35.05^\circ$  (JCPDS 40-1290 and 43-1027).

### 3.6. XPS analysis

In order to obtain the valence states of the catalysts after catalytic oxidation, three samples of Mo-Ru-Mn catalysts were analyzed with XPS technique. The results are shown in Fig. 8 and the binding energies of C 1s, Mn 2p, Mo 3d, Ru 3d, O 1s, Cl 2p and Hg 4f are listed in Table 1.

As shown in Fig. 8, the XPS results show that the Mn 2p peaks were not clearly changed after modified. The Mn  $2p_{3/2}$  spectra in these samples indicated two peaks at 642.5 and 641.5 eV (listed in Table 1). By comparison with the Mn 2p XPS spectrum database in the NIST [17],  $\text{MnO}_x$  in these samples were determined to be mainly present in the states of Mn (IV) and Mn (III). The XPS spectra data showed that Mn (II) cation was not present. It was in good agreement with the XRD results.

The Mo 3d XPS spectra exhibited three characteristic peaks, including BEs of 232.5 eV, 235.8 eV and 230.8 eV. The former two

**Table 1**  
XPS spectra data of C 1s, Mn 2p, Mo 3d, Ru 3d, O 1s, Cl 2p and Hg 4f.

Samples	Binding energy (eV)								
	C 1s	Mn 2p <sub>3/2</sub>	Mo 3d <sub>5/2</sub>	Mo 3d <sub>3/2</sub>	Ru 3d <sub>5/2</sub>	O 1s	Hg 4f <sub>5/2</sub>	Hg 4f <sub>7/2</sub>	Cl 2p
a	284.6	642.5 641.4	232.5 230.8	235.8	280.7	532.5 530.6 529.8	–	–	–
b	284.5	642.5 641.7	232.4 230.5	235.8	280.7	532.3 530.6 529.6	104.5	100.8	–
c	284.7	642.7 641.5	232.6 230.9	235.8	280.8	532.4 530.8 529.6	–	101.6	198.7

peaks were attributed to Mo (VI), and the latter one corresponded to Mo (IV). The ratio of Mo (VI) to Mo (IV) in the samples b and c had little change, compared with that in the fresh catalysts. Based on the XPS data of Mn and Mo-Ru-Mn catalysts, the peak area ratio of Mn (IV) to Mn (III) had a slight increase after Mn catalyst was modified, with the value increased from 1.63 to 2.52 (shown in Table 1).

The O 1s spectra (shown in Fig. 9) of the three catalysts showed three fitted O 1s peaks, including O<sub>a</sub> (mainly attributed to Al<sub>2</sub>O<sub>3</sub>, including little hydroxyl groups), O<sub>b</sub> (mainly attributed to RuO<sub>2</sub>, Mn<sub>2</sub>O<sub>3</sub> and lattice oxygen O<sub>d</sub>) and O<sub>c</sub> (mainly attributed to MnO<sub>2</sub>, MoO<sub>x</sub> and chemisorbed O<sub>e</sub>) [18]. Noticeably, the peak area of O 1s slightly increased after modified with Mo and Ru.

Fig. 10(b) shows that the Hg 4f spectrum of the sample b showed two peaks of 104.5 and 100.8 eV. Combined with the spectra of Hg 4f and O 1s, it can be confirmed that Hg speciation was assigned to HgO by the NIST XPS database [17]. However, the spectrum of the catalyst c was different from that of the sample b shown in Fig. 10(c). It had only one peak at 101.6 eV. Considering the spectra of Cl 2p and the BE of 101.6 eV (Hg 4f<sub>7/2</sub>), it can be confirmed that mercury was present in its bivalent state (HgCl<sub>2</sub>) on the surface of the Mo-Ru-Mn catalyst after HCl was used.

The XPS spectrum (BE 281.9 eV) of ruthenium chloride was not observed. It indicates that almost all RuCl<sub>3</sub> were activated, which was in accordance with the above results of the EDX. The BEs of ruthenium and oxygen (Ru 3d<sub>5/2</sub> at 280.7 eV and O 1s at 529.7 eV) were the characteristic of polycrystalline RuO<sub>2</sub> [26] and were identical to those in the fresh and used catalysts. The result was consistent with previous studies [24].

## 4. Discussion

### 4.1. Catalytic performance

Compared with the data shown in Fig. 2, the results indicated the catalytic performance of the MDCOs can be enhanced obviously for Hg<sup>0</sup> conversion with the addition of Mo or Ru. The efficiency was increased to 95% with Mo-Ru-Mn catalyst vs 68% for just with Mn catalyst at 423 K. The analysis of speciation for Hg after catalytic oxidation showed that there was mainly mercury (II) chloride on the surface of Mo-Ru-Mn catalyst. The distinctive difference between the unmodified and modified catalysts after contacting HCl was the obvious increase of chlorine in the latter as shown in Fig. 6. Besides, combined with the XPS analysis of spectra of Cl 2p and Hg 4f (shown in Table 1 and Fig. 10), there were much more amount of mercury (II) chloride on the surface of Mo-Ru-Mn catalyst. It was suggested that the atomic chlorine ([Cl]<sup>\*</sup>) produced from the Deacon process played a critical role during the process of Hg<sup>0</sup> conversion. Thus, the function of [Cl]<sup>\*</sup> is supposed to be able to accelerate and improve the conversion of Hg<sup>0</sup> to Hg<sup>2+</sup>.

To further verify the effect of [Cl]<sup>\*</sup> on Hg<sup>0</sup> removal, a test was carried out with 0.5 ppmv Cl<sub>2</sub> (employed concentration in the simulated flue gas) as a substitute for HCl. The Cl<sub>2</sub> concentration of

0.5 ppmv was equal in the amount of Cl<sub>2</sub> produced from the Deacon process with 8 ppmv HCl. The results indicate that the mean efficiency of three replicate tests was below 50%, far less than that in the presence of HCl. The results further verified the activity of [Cl]<sup>\*</sup> or the Deacon process in the MDCOs.

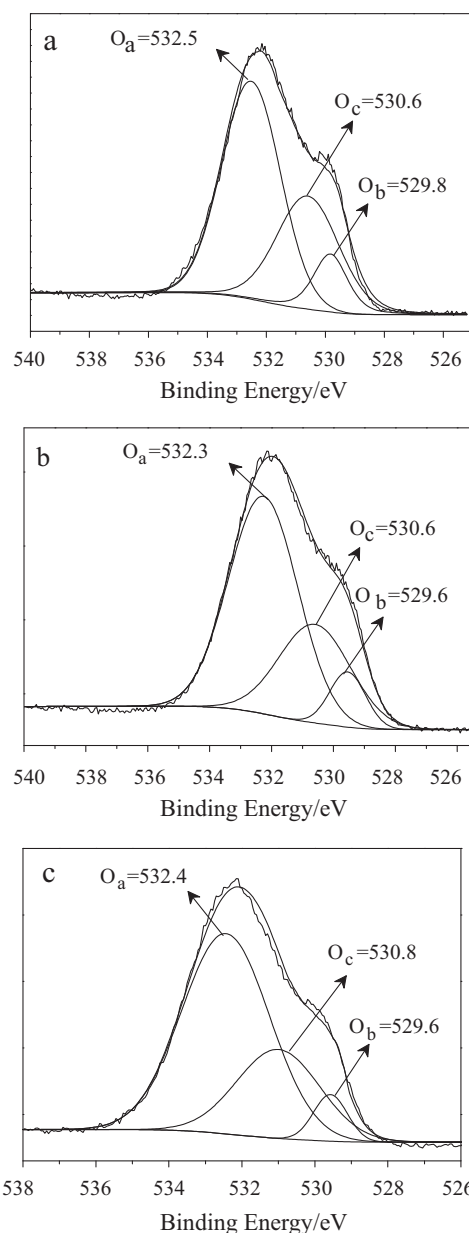


**Fig. 9.** O 1s XPS narrow scan spectra of Mo-Ru-Mn catalyst. (a) Sample a, (b) sample b and (c) sample c.

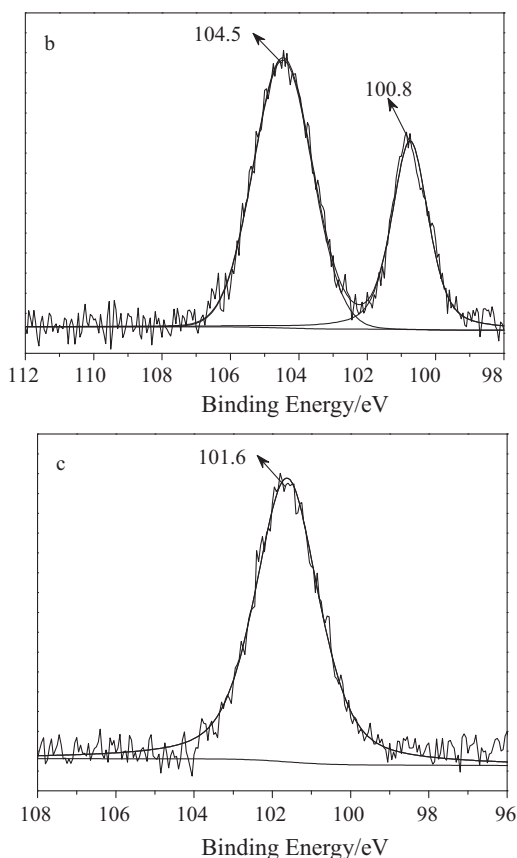


**Fig. 10.** Hg XPS spectroscopes of the Mo-Ru-Mn catalyst (dash is fitted results). (b) Sample b and (c) sample c.

The reaction between adsorbed  $\text{Hg}_{(\text{ad})}$  and  $\text{O}_2$  (resulting in the formation of  $\text{HgO}$ ) occurs at the temperature of 423 K [10]. However, the reaction process of  $\text{Hg}_{(\text{ad})}$  and  $[\text{Cl}]^{\cdot}$  has low energy barrier at room temperature, which is close to the collision limitation. Its Gibbs free energy at 423 K is highly negative, and its rate constant shows little temperature dependence [27]. An average rate constant for this reaction,  $1.5 \times 10^{13} \text{ cm}^3 \text{ mol}^{-1} \text{ s}^{-1}$ , was suggested by Senior et al. [28]. So based on the spectrum database of Hg 4f XPS (Fig. 10(b)), it can be deduced that the formation of  $\text{HgO}$  was existent, although it may not be the main production.

From Fig. 5(b), it can be seen that the addition of transition metals, especially Ru, improved greatly the conversion of HCl to  $\text{Cl}/\text{Cl}_2$ , resulting in the increase of the proportion of mercury (II) chloride. The results indicate that the addition of transition metals changed obviously the speciation of Hg after catalytic oxidation. Therefore, it is evident that the Deacon process played an important role during the process of  $\text{Hg}^0$  conversion. The results further confirmed the higher efficiencies of the MDCOs with Mo-Ru-Mn catalyst at low temperature.

Fig. 5(a) shows that most of injected HCl were retained in the MDCOs, which would be helpful to the sequential reactions for  $\text{Hg}^0$  oxidation. Therefore, the retainability for oxidants and the mode of mass delivery in the MDCOs had a notable advantage for both the conversion of HCl and the conversion efficiency of oxidants. This can be used to partly explain the higher efficiency for  $\text{Hg}^0$  removal and utilization for oxidants in the MDCOs.

That the conversion of HCl to  $\text{Cl}_2$  was rather effective in the MDCOs, can be tentatively explained from the following aspects. Firstly, the concentration of adsorbed HCl on the surface of the catalysts in the MDCOs was supposed to be higher by far than that in the TCO mode [11], accordingly, the rate of  $\text{Cl}_2$  produced from the

Deacon process became rapid. Secondly, HCl could be adequately exposed to the catalysts as it was delivered across the porous wall of the membrane, resulting in the occurrence of the Deacon process.

Fig. 4 indicates that the addition of Mo and Ru was beneficial to the MDCOs ability for sulfur-tolerance. The previous results indicated that the amount of  $\text{SO}_2$  adsorbed on the surface of catalysts decreased dramatically in the MDCOs, compared with that in the TCO mode with HCl being present [11].

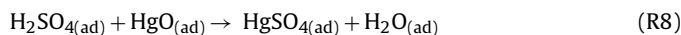
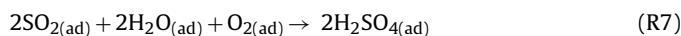
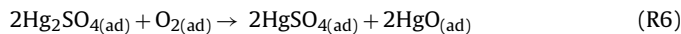
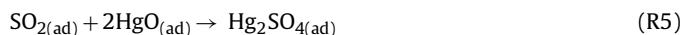
Fig. 4 shows that the addition of Mo on Mn-base material greatly increased the removal efficiencies of  $\text{Hg}^0$  and the efficiencies almost doubled compared to that in the presence of only Mn. The results and our previous studies all indicate that the larger affinity of Mo to sulfur would minimize the chance of the contact between sulfur and Mn, which was very beneficial for decreasing the deactivation or the coverage by  $\text{SO}_2$  for Mn-base active sites [13]. Meanwhile, the affinity of Mo to sulfur could diminish the competitive adsorption between  $\text{SO}_2$  and  $\text{Hg}^0$  on active sites to some extent, which would result in the increase of removal efficiency by adsorption. Fig. 4 also confirms the above results, i.e., the addition of Mo had obvious exhibition for sulfur-tolerance, which would promote the contact between whether  $\text{Hg}^0$  and Mn-base active sites or the catalysts and oxidants. Moreover, the HCl delivery mode in the MDCOs ensures its exposure to the catalyst preferentially. Therefore the Deacon process was accelerated because of preferential contact between oxidants and catalysts. All these improved the ability of the MDCOs for sulfur-tolerance, resulting in the occurrence of high removal of  $\text{Hg}^0$  in the MDCOs, compared with that in the TCO mode.

Fig. 4 also shows obviously that the presence of  $\text{SO}_2$  suppressed  $\text{Hg}^0$  removal. However, the influence of  $\text{SO}_2$  was insignificant. The influence of  $\text{SO}_2$  on the removal of  $\text{Hg}^0$  can be analyzed from the following aspects. Firstly, when  $\text{SO}_2$  contacted with the catalysts, it would be adsorbed on the surface and active sites of the catalysts, resulting in the competitive adsorption for catalyst active sites between HCl and  $\text{SO}_2$  or  $\text{SO}_2$  and  $\text{Hg}^0$ . Secondly, the Deacon process was interfered by the competitive adsorption. This may be the main cause for reducing the efficiencies of the MDCOs. Thirdly,  $\text{HgSO}_{4(\text{ad})}$  could be formed and was too tightly adsorbed on the surface of the catalysts to escape along with flue gas, which hampered the adsorption of the catalysts for  $\text{Hg}^0$ , resulting in the decline of  $\text{Hg}^0$  removal.

The previous studies have shown that the  $\text{Al}_2\text{O}_3$  support can be sulfated upon  $\text{SO}_2$  adsorption [29].  $\text{SO}_2$  strongly chemisorbs at basic surface hydroxyls and  $\text{O}^{2-}$  sites, resulting in the formation of adsorbed (bi) sulfites, which can be converted to sulfates upon oxidation. Due to the formation of sulfate on the surface of the catalysts, there might be the sulfation of active phase, e.g.,  $\text{MnSO}_4$ . The sulfation of Mn-base active phase would result in the decreased efficiency of the Deacon reaction. The test also found the presence of  $\text{HgSO}_4$ , which might inhibit the Deacon reaction and adsorption of  $\text{Hg}^0$  on the active sites because of the firm combination between the sulfate and active phase.

The formation of  $\text{HgSO}_4$  could occur through two pathways at the test conditions. One was that  $\text{SO}_2$  firstly reacted with  $\text{HgO}$  to form  $\text{Hg}_2\text{SO}_4$ , and then  $\text{Hg}_2\text{SO}_4$  was converted to  $\text{HgSO}_4$  upon oxidation. Another was that  $\text{SO}_2$  reacted firstly with  $\text{H}_2\text{O}_{(\text{ad})}$  to form  $\text{H}_2\text{SO}_4$ , and then  $\text{H}_2\text{SO}_4$  reacted with  $\text{HgO}$  to form  $\text{HgSO}_4$ . Based on the test results, the former process could be achieved. However, the latter might be present when air was used as carrier gas. Based on the analysis above, the reaction pathway could be written as:





Besides the inhibition for  $\text{Hg}^0$  removal by  $\text{HgSO}_4$ , based on the previous literatures [30],  $\text{SO}_2$  had an inhibitory effect on homogeneous oxidation of  $\text{Hg}^0$  by combination with Cl-base, resulting in the decreased efficiency of reactive activated chlorine.

#### 4.2. Redox behaviors

It is usually considered that the capture of elemental mercury mainly occurs via a Mars–Maessen redox mechanism [3,9,27,31]. In this mechanism,  $\text{Hg}^0$  firstly absorbed on the surface of the catalysts and then reacted with the lattice oxygen to form  $\text{HgO-MO}_x$ . It was reported that certain  $\text{Hg}^0$  removal efficiencies could be found and decreased in the absence of  $\text{O}_2$ . After introducing  $\text{O}_2$ , the  $\text{Hg}^0$  removal efficiencies recovered again [31]. The XPS results presented above also indicated that  $\text{Hg}^0$  was oxidized to mercury oxide by the Mn-base catalysts in the presence of gaseous oxygen, supporting the Mars–Maessen mechanism.

The phase of Mn had a critical role on the conversion of  $\text{Hg}^0$  in this test. The XRD results show the presence of mixed  $\text{MnO}_2$  and  $\text{Mn}_2\text{O}_3$  phases on the surface of the fresh catalysts. The test also showed that the ratio of Mn (IV) to Mn (III) decreased greatly after catalytic oxidation under the condition of high pure  $\text{N}_2$ . On the contrary, according to Fig. 8, the ratio of Mn (IV) to Mn (III) increased markedly after modified. So it can be concluded that the reduced Mn (IV) could be completely regenerated during the process of the reaction with air as carrier gas. The results could be used to partly explain the reason why the Mo–Ru–Mn catalyst showed excellent catalytic activity at low temperature.

According to Fig. 8, the ratio of Mo (VI) to Mo (IV) on the surface of catalysts before and after catalytic oxidation had little change. The valence state of Ru was identical to the fresh and used catalysts and presented in the form of Ru (IV). It indicates that the Deacon process unaltered practically the state of Mo, especially Ru, which highlighted the stability of the catalysts [26,32]. Moreover, it is thought that mercury oxidation with HCl requires the assistance of  $\text{O}_2/\text{O}$ , and the Deacon reaction also needs the ambience of  $\text{O}_2/\text{O}$ . So, the above results show clearly that  $\text{O}_2$  played a crucial role in stabilizing the speciation of the catalysts, improving the efficiency of the Deacon reaction and promoting the oxidation of  $\text{Hg}^0$ .

During the process of the oxidation of  $\text{Hg}^0$ , the exhausted lattice oxygen of the catalysts could be supplied by the gas-phase oxygen [3,27,31]. Fig. 9 indicates that the oxygen content (mainly from  $\text{O}_d$  and  $\text{O}_e$ ) on the surface of the catalysts increased after modified. The result was beneficial to both the regeneration of transition metal oxides and the conversion of  $\text{Hg}^0$ . The reasons could be explained from the following two aspects. On the one hand,  $\text{O}_d$  and  $\text{O}_e$  (derived from adsorbed oxygen  $\text{O}_{2(\text{ad})}$ ) on the surface of the catalysts would be helpful to the reduction of Mn (III) to Mn (IV), and the reduction of Mo (IV) to Mo (VI). On the other hand, the reaction between  $\text{O}_{2(\text{ad})}$  and adsorbed  $\text{Hg}^0$  ( $\text{Hg}_{(\text{ad})}$ ) could be promoted to some extent. The results were consistent with the literatures [27,31].

## 5. Conclusions

The catalytic activities of the MDCOs system for conversion of  $\text{Hg}^0$  to  $\text{Hg}^{2+}$  were examined with different transition metals as catalysts at low temperature of 423 K. The results show that the conversion efficiencies of  $\text{Hg}^0$  were largely improved with modified catalysts in the presence of 8 ppmv HCl. Mo–Ru–Mn catalyst had

excellent performance during the process of  $\text{Hg}^0$  conversion and the Deacon reaction. The experiment also indicated that the species of transition metals of Mn, Mo and Ru were mainly  $\text{MnO}_2$ ,  $\text{MoO}_3$  and  $\text{RuO}_2$ , respectively, according to the XRD and XPS analysis. After modified with Mo and Ru, Mn catalyst had better performance for chlorine yield and sulfur-tolerance to  $\text{SO}_2$ .

In addition, the high removal efficiency of  $\text{Hg}^0$  was mainly attributed to the formation of activated  $[\text{Cl}]^*$  derived from the Deacon process. Compared with the TCO mode, the MDCOs had absolute predominance at the conversion of  $\text{Hg}^0$ , improvement of the Deacon process, ability of sulfur-tolerance, catalytic activity of catalysts and utilization of oxidants.

## Acknowledgment

This work was supported by NSFC Project (21077073) and the High-Tech R&D Program of China (863) under grant no. 2011AA060801.

## References

- [1] S.X. Wang, L. Zhang, G.H. Li, Y. Wu, J.M. Hao, N. Pirrone, F. Sprovieri, M.P. Ancora, Mercury emission and speciation of coal-fired power plants in China, *Atmos. Chem. Phys.* 10 (2010) 1183–1192.
- [2] J.H. Pavlish, L.L. Hamre, Y. Zhuang, Mercury control technologies for coal combustion and gasification systems, *Fuel* 89 (2010) 838–847.
- [3] M.H. Kim, S.W. Ham, J.B. Lee, Oxidation of gaseous elemental mercury by hydrochloric acid over  $\text{CuCl}_2/\text{TiO}_2$ -based catalysts in SCR process, *Appl. Catal. B* 99 (2010) 272–278.
- [4] S.H. Wu, S.A. Wang, J.H. Gao, Y.Y. Wu, G.Q. Chen, Y.W. Zhu, Interactions between mercury and dry FGD ash in simulated post combustion conditions, *J. Hazard. Mater.* 188 (2011) 391–398.
- [5] S. He, J.S. Zhou, Y.Q. Zhu, Z.Y. Luo, M.J. Ni, K.F. Cen, Mercury oxidation over a vanadia-based selective catalytic reduction catalyst, *Energy Fuel* 23 (2009) 253–259.
- [6] H. Kamata, S. Ueno, N. Sato, T. Naito, Mercury oxidation by hydrochloric acid over  $\text{TiO}_2$  supported metal oxide catalysts in coal combustion flue gas, *Fuel Process. Technol.* 90 (2009) 947–951.
- [7] S. Straube, T. Hahn, H. Koeser, Adsorption and oxidation of mercury in tail-end SCR–DeNO<sub>x</sub> plants—Bench scale investigations and speciation experiments, *Appl. Catal. B* 79 (2008) 286–295.
- [8] A.A. Presto, E.J. Granite, Noble metal catalysts for mercury oxidation in utility flue gas gold, palladium and platinum formulations, *Platinum Met. Rev.* 52 (2008) 144–154.
- [9] W.J. Lee, G.N. Bae, Removal of elemental mercury ( $\text{Hg}^0$ ) by nanosized  $\text{V}_2\text{O}_5/\text{TiO}_2$  catalysts, *Environ. Sci. Technol.* 43 (2009) 1522–1527.
- [10] B. Hall, P. Sehager, O. Lindqvist, Chemical reactions of mercury on combustion flue gases, *Water, Air, Soil Pollut.* 56 (1991) 3–14.
- [11] Y.F. Guo, N.Q. Yan, S.J. Yang, Z. Qu, Z.B. Wu, Y. Liu, P. Liu, J.P. Jia, Conversion of elemental mercury with a novel membrane delivery catalytic oxidation system (MDCOs), *Environ. Sci. Technol.* 45 (2011) 706–711.
- [12] S.H. Qiao, J. Chen, J.F. Li, Z. Qu, P. Liu, N.Q. Yan, J.P. Jia, Adsorption and catalytic oxidation of gaseous elemental mercury in flue gas over  $\text{MnO}_x/\text{alumina}$ , *Ind. Eng. Chem. Res.* 48 (2009) 3317–3322.
- [13] J.F. Li, N.Q. Yan, Z. Qu, S.H. Qiao, S.J. Yang, Y.F. Guo, P. Liu, J.P. Jia, Catalytic oxidation of elemental mercury over the modified catalyst Mn/ $\alpha\text{-Al}_2\text{O}_3$  at lower temperatures, *Environ. Sci. Technol.* 44 (2010) 426–431.
- [14] X.P. Fan, C.T. Li, G.M. Zeng, Z. Gao, L. Chen, W. Zhang, H.L. Gao, Removal of gas-phase elemental mercury by activated carbon fiber impregnated with  $\text{CeO}_2$ , *Energy Fuel* 24 (2010) 4250–4254.
- [15] S.S. Lee, J.Y. Lee, T.C. Keener, Bench-scale studies of in-duct mercury capture using cupric chloride-impregnated carbons, *Environ. Sci. Technol.* 43 (2009) 2957–2962.
- [16] E.J. Granite, H.W. Pennline, Photochemical removal of mercury from flue gas, *Ind. Eng. Chem. Res.* 41 (2002) 5470–5476.
- [17] NIST XPS Database, <http://srdata.nist.gov/xps/> (accessed August 2007).
- [18] T.T. Gu, Y. Liu, X.L. Weng, H.Q. Wang, Z.B. Wu, The enhanced performance of ceria with surface sulfation for selective catalytic reduction of NO by  $\text{NH}_3$ , *Catal. Commun.* 12 (2010) 310–313.
- [19] K.C. Galbreath, C.J. Zygarlicke, Mercury transformations in coal combustion flue gas, *Fuel Process. Technol.* 65 (2000) 289–310.
- [20] H.Y. Pan, R.G. Minet, S.W. Benson, T.T. Tsotsis, Process for converting hydrogen chloride to chlorine, *Ind. Eng. Chem. Res.* 33 (1994) 2996–3003.
- [21] J.P. Hofmann, S. Zweidinger, M. Knapp, A.P. Seitsonen, K. Schulte, J.N. Andersen, E. Lundgren, H. Over, Hydrogen-promoted chlorination of  $\text{RuO}_2(110)$ , *J. Phys. Chem. C* 114 (2010) 10901–10909.
- [22] S. Zweidinger, J.P. Hofmann, O. Balmes, E. Lundgren, H. Over, In situ studies of the oxidation of HCl over  $\text{RuO}_2$  model catalysts: stability and reactivity, *J. Catal.* 272 (2010) 169–175.



- [23] Y. Li, P. Murphy, C.Y. Wu, Removal of elemental mercury from simulated coal-combustion flue gas using a SiO<sub>2</sub>-TiO<sub>2</sub> nanocomposite, *Fuel Process. Technol.* 89 (2008) 567–573.
- [24] V. Mazziari, F. Coloma-Pascual, A. Arcoya, P. L'Argentiere, N.S. Figoli, XPS, FTIR and TPR characterization of Ru/Al<sub>2</sub>O<sub>3</sub> catalysts, *Appl. Surf. Sci.* 210 (2003) 222–230.
- [25] J.H. Li, X. Liang, S.C. Xu, J.M. Hao, Catalytic performance of manganese cobalt oxides on methane combustion at low temperature, *Appl. Catal. B* 90 (2009) 307–312.
- [26] N. Lopez, J. Gomez-Segura, R.P. Marin, J. Perez-Ramirez, Mechanism of HCl oxidation (Deacon process) over RuO<sub>2</sub>, *J. Catal.* 255 (2008) 29–39.
- [27] P. Fang, C.P. Cen, D.S. Chen, Z.X. Tang, Carbonaceous adsorbents prepared from sewage sludge and its application for Hg<sup>0</sup> adsorption in simulated flue gas, *Chin. J. Chem. Eng.* 18 (2010) 231–238.
- [28] C.L. Senior, A.F. Sarofim, T.F. Zeng, J.J. Helble, R. Mamani-Paco, Gas-phase transformations of mercury in coal-fired power plants, *Fuel Process. Technol.* 63 (2000) 197–213.
- [29] W.S. Kijlstra, M. Biervliet, E.K. Poels, A. Bliet, Deactivation by SO<sub>2</sub> of MnO<sub>x</sub>/Al<sub>2</sub>O<sub>3</sub> catalysts used for the selective catalytic reduction of NO with NH<sub>3</sub> at low temperatures, *Appl. Catal. B* 16 (1998) 327–337.
- [30] H. Agarwal, H.G. Stenger, S. Wu, Z. Fan, Effects of H<sub>2</sub>O, SO<sub>2</sub>, and NO on homogeneous Hg oxidation by Cl<sub>2</sub>, *Energy Fuel* 20 (2006) 1068–1075.
- [31] Y. Liu, Y.J. Wang, H.Q. Wang, Z.B. Wu, Catalytic oxidation of gas-phase mercury over Co/TiO<sub>2</sub> catalysts prepared by sol-gel method, *Catal. Commun.* 12 (2011) 1291–1294.
- [32] D. Crihan, M. Knapp, S. Zweidingey, E. Lundgren, C.J. Weststrate, J.N. Andersen, A.P. Seitsonen, H. Over, Stable Deacon process for HCl oxidation over RuO<sub>2</sub>, *Angew. Chem. Int. Ed.* 47 (2008) 2131–2134.